Bioorganic Chemistry 114 (2021) 105114

Contents lists available at ScienceDirect

Bioorganic Chemistry

journal homepage: www.elsevier.com/locate/bioorg

Synthesis of 1,4-dihydropyrazolo[4,3-*b*]indoles via intramolecular C(sp^2)-N bond formation involving nitrene insertion, DFT study and their anticancer assessment

Manpreet Kaur [a], Vikrant Mehta [b], Aabid Abdullah Wani [c], Sahil Arora [a], Prasad V. Bharatam [c], Ashoke Sharon [d], Sandeep Singh [b,*], Raj Kumar [a,*]

[a] *Laboratory for Drug Design and Synthesis, Department of Pharmaceutical Sciences and Natural Products, School of Pharmaceutical Sciences, Central University of Punjab, Bathinda-151401, Punjab, India*
[b] *Department of Human Genetics and Molecular Medicine, Central University of Punjab, Bathinda-151401, Punjab, India*
[c] *Department of Medicinal Chemistry, National Institute of Pharmaceutical Education and Research (NIPER), SAS. Nagar, India*
[d] *Department of Chemistry, Birla Institute of Technology, Mesra, Ranchi, Jharkhand, 835215, India*

ARTICLE INFO

Keywords:
1,4-Dihydropyrazolo[4,3-*b*]indoles
C—N bond formation
Cadogan Cyclization
DFT study
Cancer
Topoisomerase inhibitors

ABSTRACT

We herein report a new synthetic route for a series of unreported 1,4-dihydropyrazolo[4,3-*b*]indoles (**6**–**8**) via deoxygenation of *o*-nitrophenyl-substituted *N*-aryl pyrazoles and subsequent intramolecular (sp^2)-N bond formation under microwave irradiation expedite modified Cadogan condition. This method allows access to NH-free as well as *N*-substituted fused indoles. DFT study and controlled experiments highlighted the role of nitrene insertion as one of the plausible reaction mechanisms. Furthermore, the target compounds exhibited cytotoxicity at low micromolar concentration against lung (A549), colon (HCT-116), and breast (MDA-MB-231, and MCF-7) cancer cell lines, induced the ROS generation and altered the mitochondrial membrane potential of highly aggressive MDA-MB-231 cells. Further investigations revealed that these compounds were selective Topo I (**6h**) or Topo II (**7a, 7b**) inhibitors.

1. Introduction

C—N bond formation [1–3] offers opportunities to construct diverse *N*-heterocycles with broader applications in pharmaceuticals,[4] supramolecular chemistry,[5] crop protecting agents,[6] etc. The majority of the C—N bond formation methods such as Buchwald-Hartwig amination reaction,[7] Ugi reaction,[8] and Eschweiler-Clarke methylation reaction[9] either utilize amines, imines or amides as one of the starting materials (nitrogen source) in the presence or absence of metal and/or ligand to access heterocyclic skeletons. The admittance to molecular diversity has amplified inspiring enthusiasm among synthetic chemists from the past decade because of its vivacious role in drug discovery. It is, therefore, of high importance to introduce efficient methods to synthesize new compounds of pharmaceutical interests. Reactions involving intramolecular reductive cyclization of o-functionalized nitroarenes using a reductant to construct heterocycles[10–11] such as carbazoles, [12] indazoles,[13] and indoles[14] are gaining significant importance as they involve the direct conversion of a nitro group into reactive nitrogen species. The Cadogan/Cadogan-Sundberg cyclization[15–16] is one of the well-studied reductive cyclization reactions for synthesizing these skeletons, and the literature is witnessed on their advancements. [1]

Cancer has been recognized as one of the major diseases which is causing mortality worldwide, thus remains a major health problem to resolve. From the last five years, almost 29% of the drugs have been approved by the US to treat various types of cancers.[17] Nowadays, to combat cancer, the anticancer treatment approach has been advanced to target-based drug discovery[18] like targeting topoisomerases (Topos), [19] epidermal growth factor receptor,[20] HDACs,[21] etc. as their overexpression mediate growth of a variety of cancers, especially lung, breast, ovary, colon, etc. Among these targets, topoisomerases, due to their role in maintaining the topology of DNA, are identified as one of

Abbreviations: CPT, Camptothecin; IC_{50}, Inhibitory Concentration at half-maximal; Topo, Topoisomerase; MTT, (3-(4,5-Dimethylthiazol-2-yl)-2,5-diphenyltetrazolium Bromide; ROS, Reactive Oxygen Species; MMP, Mitochondrial Membrane Potential.

* Corresponding authors.
E-mail addresses: sandeepsingh82@cup.edu.in, sandeepsingh82@gmail.com (S. Singh), raj.khunger@gmail.com, rajcps@cup.edu.in (R. Kumar).

https://doi.org/10.1016/j.bioorg.2021.105114
Received 27 April 2021; Received in revised form 17 June 2021; Accepted 18 June 2021
Available online 29 June 2021

the most important cellular targets for clinically potent anticancer agents.[22]

Indoles are attractive molecules due to their ubiquity in nature.[5,23–24] Heteroaryl-substituted or fused-indoles epitomize privileged architectural units frequently found in pharmaceuticals and bioactive molecules.[25] Sunitinib, indomethacin, pindolol, physostigmine, delavirdine, metralindole, vincristine, and sumatriptan are some of the FDA approved indole containing drugs for the treatment of cancer, cardiovascular and neurologic disorders (Fig. 1).[26]

Recently carbazoles, pyrazolocarbazoles and *N*-acetyl pyrazolines (Fig. 2) have emerged as potent anticancer agents via topoisomerase inhibition as one of their primary targets.[27–29] Considering the structural scaffolds of the compounds as mentioned above, we designed new 1,4-dihydropyrazolo[4,3-*b*]indoles as Topo I/II inhibitors based on merging of active pharmacophores and their preliminary docking (**6 h**; a representative compound) into the proteins, which rationalized their proposed inhibitory activity.

It was surprising to know that only a few synthetic methods to access pyrazolo[4,3-*b*] or [3,4-*b*]indole derivatives have been developed during the past decade (Scheme 1a-c). These involve either intramolecular palladium-catalyzed Heck-type heteroarylation of o-bromoanilinopyrazoles (Scheme 1a),[30] gold-catalyzed three-component annulation reaction of alkynes, hydrazines and ketone/aldehydes (Scheme 1b),[31] or a three-step one-pot process consisting of the iodination of indole-2-carbaldehyde under basic conditions, followed by hydrazone formation and intramolecular cross-coupling using copper iodide (Scheme 1c).[32] Besides, none of the methods offers an inexpensive methodology with diverse substitutions at N-1, C-3 and N-4 positions of 1,4-dihydropyrazolo[4,3-*b*]indoles.

We report herein the synthesis of unreported 1,4-dihydropyrazolo [4,3-*b*] indoles (**6**) and their derivatives (**7** and **8**) via intramolecular reductive cyclization of 5-(o-nitroaryl)-1,3-diaryl-1*H*-pyrazole (**5**) under modified-Cadogan conditions in the presence of a reductant (trivalent phosphorus) and with or without an electrophile (BnCl) under microwave irradiations (Scheme 1d) along with DFT studies and their anticancer assessment.

2. Results and discussions

2.1. Chemistry

2.1.1. Optimisation of reaction conditions

To begin with, nitro-substituted precursors (**5a-5j**) were synthesized (Scheme S1; see supplementary material file) as per the methodology reported by our research group.[33] To determine the standard reaction conditions for the synthesis of target compounds, **5d** was chosen as the model substrate. The standard Cadogan reaction conditions were selected that employ reductant, i.e. PPh_3 (3 equiv; method A) or $P(OEt)_3$ (3 equiv; method B) to carry out exhaustive deoxygenation of **5d** (1 equiv) in different solvents at high temperature (Table 1).

The initial screening revealed that **6d** was solely obtained (61%; entry 3, Table 1) under method A in carrying out the reaction of **5d** in toluene at 180 °C for 20 min under MW, whereas method B yielded **6d** (52%) along with **7d** (18%) when **5d** was heated under MW in toluene at 210 °C for 30 min (entry 12, Table 1). Reactions under solvent-free conditions failed to afford the desired products in method A or B (entries 1, 9 and 10, Table 1). Microwave heating of reaction[34] was found to accelerate the reaction rate and increase the yield in both the methods (compare entry 2 with 3; compare entry 11 with 12, Table 1) except under neat conditions. Further, non-polar solvent, particularly toluene, emerged as the best choice for both the methods amidst solvents such as 1,4-dioxane, DMF, CH_3CN, MeOH and water. Unexpectedly, *N*-ethoxy product (**9d**) was not obtained with method B, which is generally observed along with NH product in $P(OEt)_3$-mediated reductive cyclization.[1] Interestingly possible formation of compounds with dibenzo [*b,f*]pyrazolo[1,5-*d*][1,4]diazepine ring system (**10d-12d**, Table 1) was

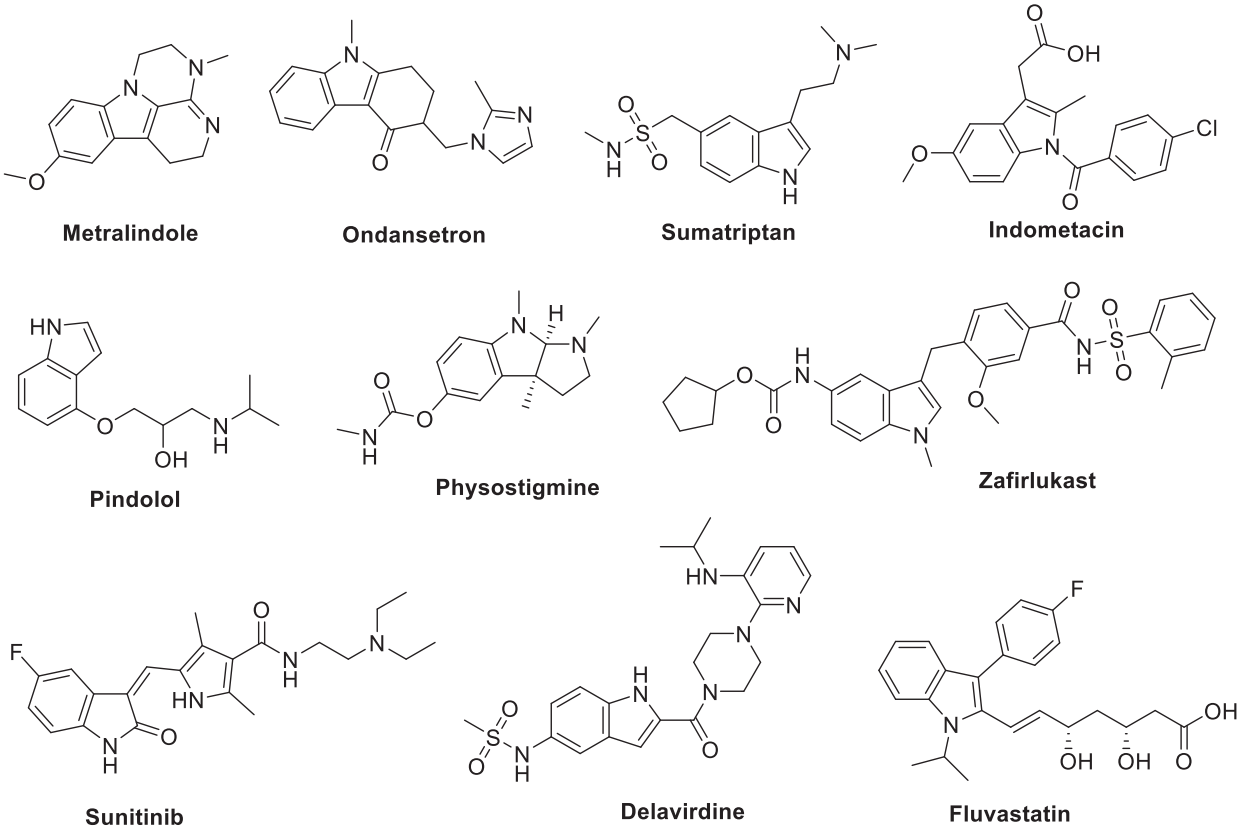

Fig. 1. Indole based FDA approved drugs.

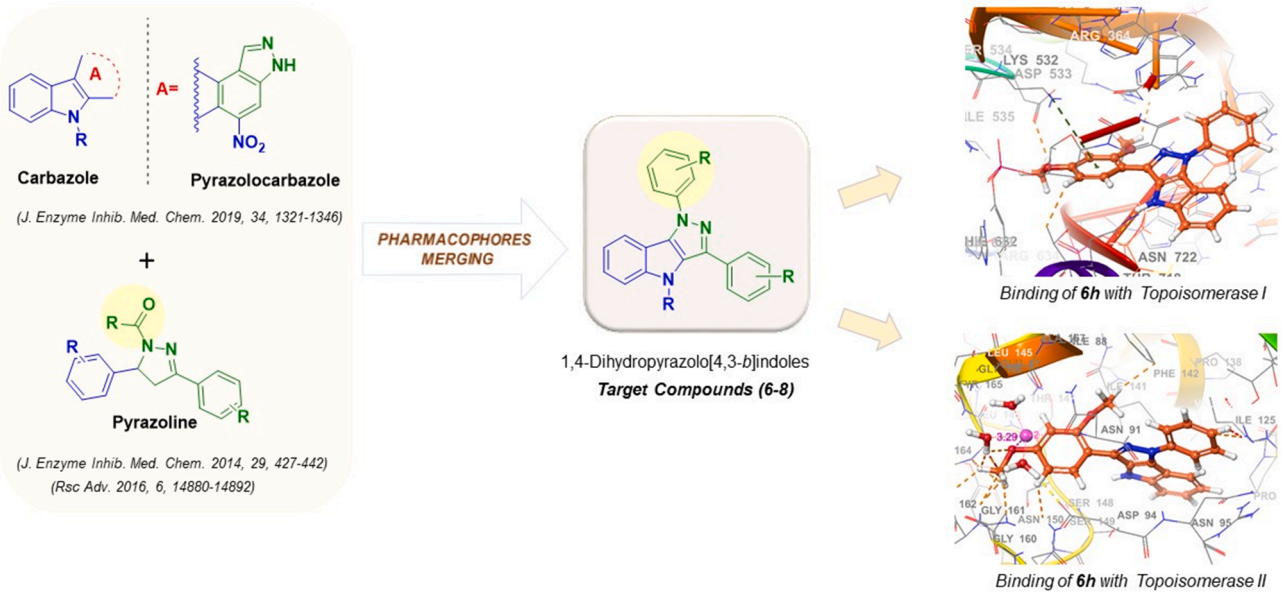

Fig. 2. Design of target compounds (**6**–**8**) as topoisomerase I/II inhibitors.

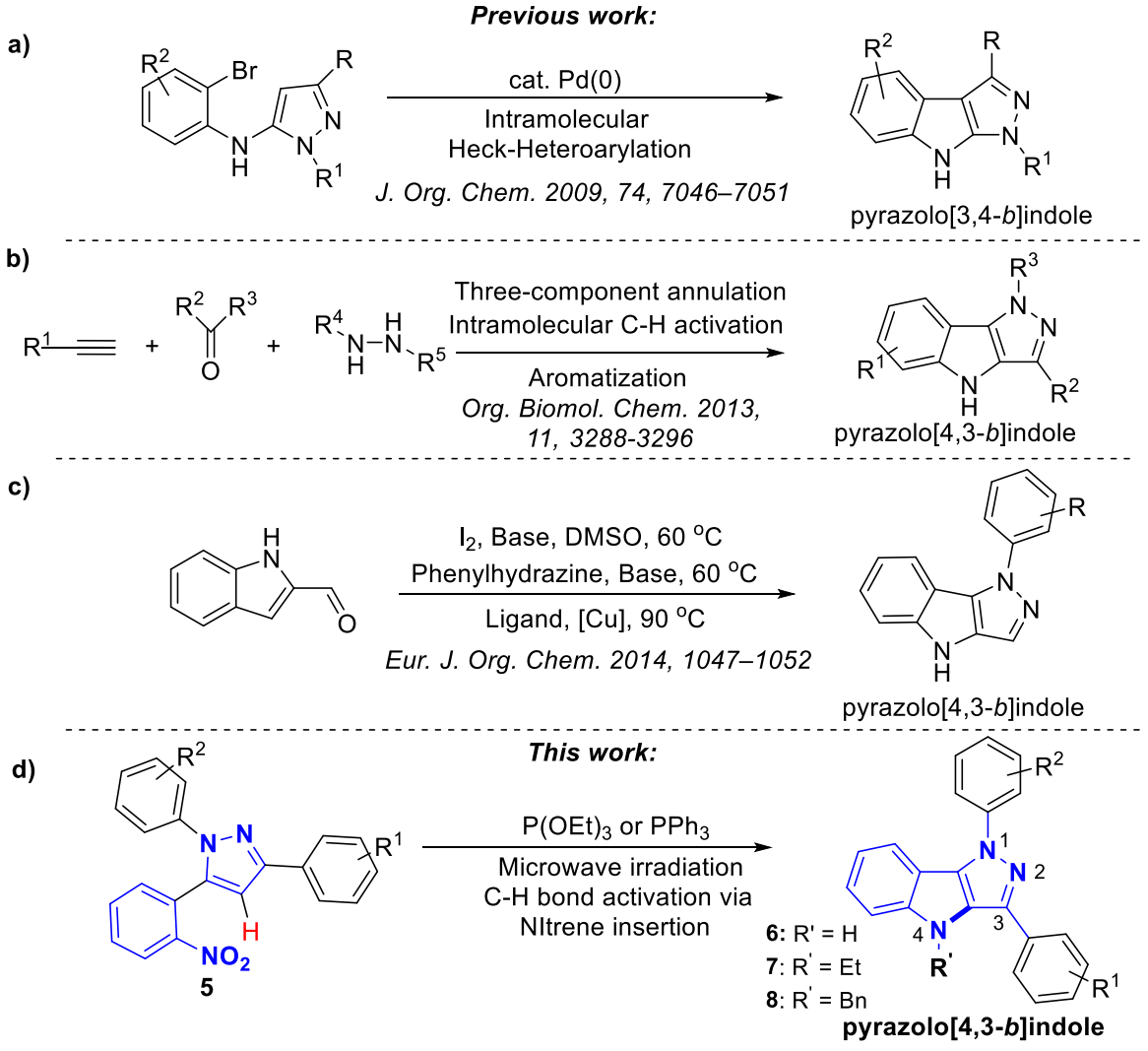

Scheme 1. Synthetic approaches for pyrazolo[4,3-*b*] or [3,4-*b*]indoles.

Table 1
Optimization of reaction conditions[a].

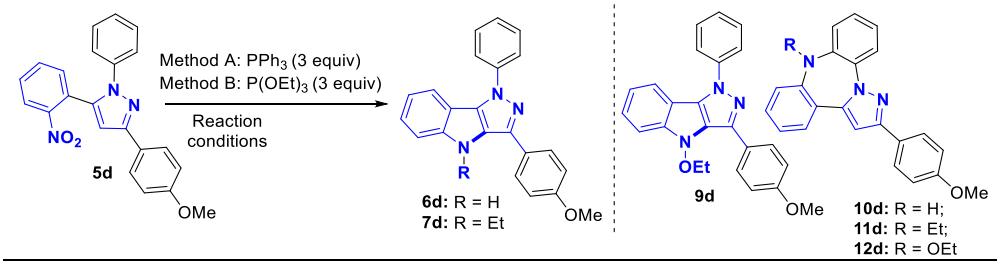

Entry	Solvent	Method	Reaction Conditions	Yield (%)[b]	
				6d	**7d**
1	–	A	180 °C, 24 h	Trace[c]	–
2	Toluene	A	Reflux, 24 h	22	–
3	Toluene	A	MW, 180 °C, 20 min	61[d]	–
4	1,4-Dioxane	A	MW, 180 °C, 20 min	49	–
5	DMF	A	MW, 180 °C, 20 min	17	–
6	CH_3CN	A	MW, 180 °C, 20 min	15	–
7	MeOH	A	MW, 180 °C, 20 min	11	–
8	H_2O	A	MW, 180 °C, 20 min	–	–
9	–	B	Reflux, 24 h	3	Trace
10	–	B	MW, 210 °C, 30 min	8	3
11	Toluene	B	Reflux, 24 h	16	9
12	Toluene	B	MW, 210 °C, 30 min	52[d]	18[d]
13	1,4-Dioxane	B	MW, 210 °C, 30 min	29	10
14	DMF	B	MW, 210 °C, 30 min	19	9
15	CH_3CN	B	MW, 210 °C, 30 min	11	6
16	MeOH	B	MW, 210 °C, 30 min	7	2
17	H_2O	B	MW, 210 °C, 30 min	–	–

[a] Substrate 5d (1 mmol, 1 equiv) was treated either with PPh_3 (3 equiv; method A) or $P(OEt)_3$ (3 equiv; method B), [b]Isolated yield, [c]reaction under MW (sealed tube) at 180 °C did not improve the yield. [d]Increase in time upto 2 h did not have much effect on the % yield.

also not detected.

To further explore the scope and limitations of reductive cyclization, nitro-substituted precursors were treated using method A or B under optimized conditions (Scheme 2a) to afford the target compounds (**6** and **7**). The reaction was found to be compatible with diverse functional groups on both the phenyl rings. For unknown reasons, corresponding products **6i** and **6j** of **5i** and **5j** were not obtained in method B.

Furthermore, the methodology was found to help construct *N*4 alkylated pyrazolo[4,3-*b*]indole *in situ*. For instance, when a mixture of **5d** (1 equiv), PPh_3 (3 equiv) and benzyl chloride (1.5 equiv) was heated under MW irradiations (sealed tube) at 180 °C for 20 min, it resulted in the formation of *N*4-benzylated product (**8d**; 61%; Scheme 2b). This further extends the scope of methodology.

2.1.2. Mechanism of reaction (DFT study)

To understand the mechanism of reaction and formation of **6** and **7** under Cadogan conditions particularly using $P(OEt)_3$ as reductant, quantum chemical studies on **5k** ($R^1 = R^2 = R^3 = R^4 = R^5 = R^6 = H$; a model substrate) were performed using Density Functional B3LYP and 6–31 + G(d) basis set (see Supplementary material).[35–37] The overall cyclization process was found to be thermodynamically favorable (Fig. 3) and exergonic by 70.59 kcal/mol, which can be seen from the free energy profile diagram (Fig. 4). The formation of products firstly involves the nucleophilic attack of the lone pair of $P(OEt)_3$ on the oxygen atom of the nitro of **5 k** followed by removal of $PO(OEt)_3$, resulting in the formation of nitroso intermediate **5 ka**.[16,38–42] Further, **5ka** changes into product **6 k** via nitrene pathway, which involves deoxygenation of nitroso intermediate by $P(OEt)_3$ followed by the release of $PO(OEt)_3$ and formation of nitrene intermediate **5 kb** (Fig. 4).

The conformational analysis of **5kb** revealed the possibility of another conformer, **5kb**−**C2**. The formation of **5kb_C2** has been found to be endergonic by 4.18 kcal/mol (Fig. 4). The activation barrier required for the formation of the O—P bond in **5kb_C2** is 70.55 kcal/mol. The quantum chemical studies suggest the activation energy needed for the formation of the O—P bond in **5kb_C2** can serve as a rate-limiting step for the formation of the product (**6k**). Two products are possible from **5kb_C2** along two different pathways (Pathway A and Pathway B; Fig. 3). Pathway A leads to the formation of *N*-OH (**6kb**) product, which is exergonic by 9.15 kcal/mol with an activation barrier of 30.39 kcal/mol, whereas Pathway B would lead to the formation of N—H (**6k**) product, which is exergonic by 78.85 kcal/mol with an activation barrier of 14.91 kcal/mol. The energetics of the two pathways and the experimental results motivated us to explore Pathway B (Fig. 3B), which involves the nitrene formation and its insertion to give the product. The formation of nitrene intermediate **5kc** from **5kb_C2** is exergonic by 5.72 kcal/mol and hence is a thermodynamically favourable process.

The cyclization process involves the insertion of nitrene into the pyrazole C—H bond, resulting in the formation of a cyclized product which is exergonic by 69.05 kcal/mol. This insertion process involves an activation barrier of 14.91 kcal/mol. The role of triethyl phosphate of **5kb** is to activate the pyrazole C—H bond, facilitating the nitrene insertion into the C—H bond of the pyrazole ring. Hence, triethyl phosphate here is analogous to iron which has been found to catalyze a similar kind of C—H activation followed by nitrene insertion and cyclization.[43].

Further, detection of a phosphorimidate byproduct in LC-MS (**15d**; Scheme S2) along with **6d**, **7d** and absence of *N*-OEt[44] product (**9d**) during a controlled experiment of **5d** with in excess of $P(OEt)_3$ confirmed that present reaction occurs possibly via a nitrene mechanism and not by [13,16] non-nitrene pathway. The formation of *N*-substituted products like *N*-ethyl (ΔG = -1.71, E_a = 68.39) (**7**) and *N*-benzyl (ΔG = 6.08, E_a = 55.10) (**8**) can be justified as the products of nucleophilic substitution reactions of (**6k**) with the $P(OEt)_3$ and benzyl chloride, respectively under given reaction conditions. All the final products were new and fully characterized (mp, NMR, HRMS and X-ray; see SI).

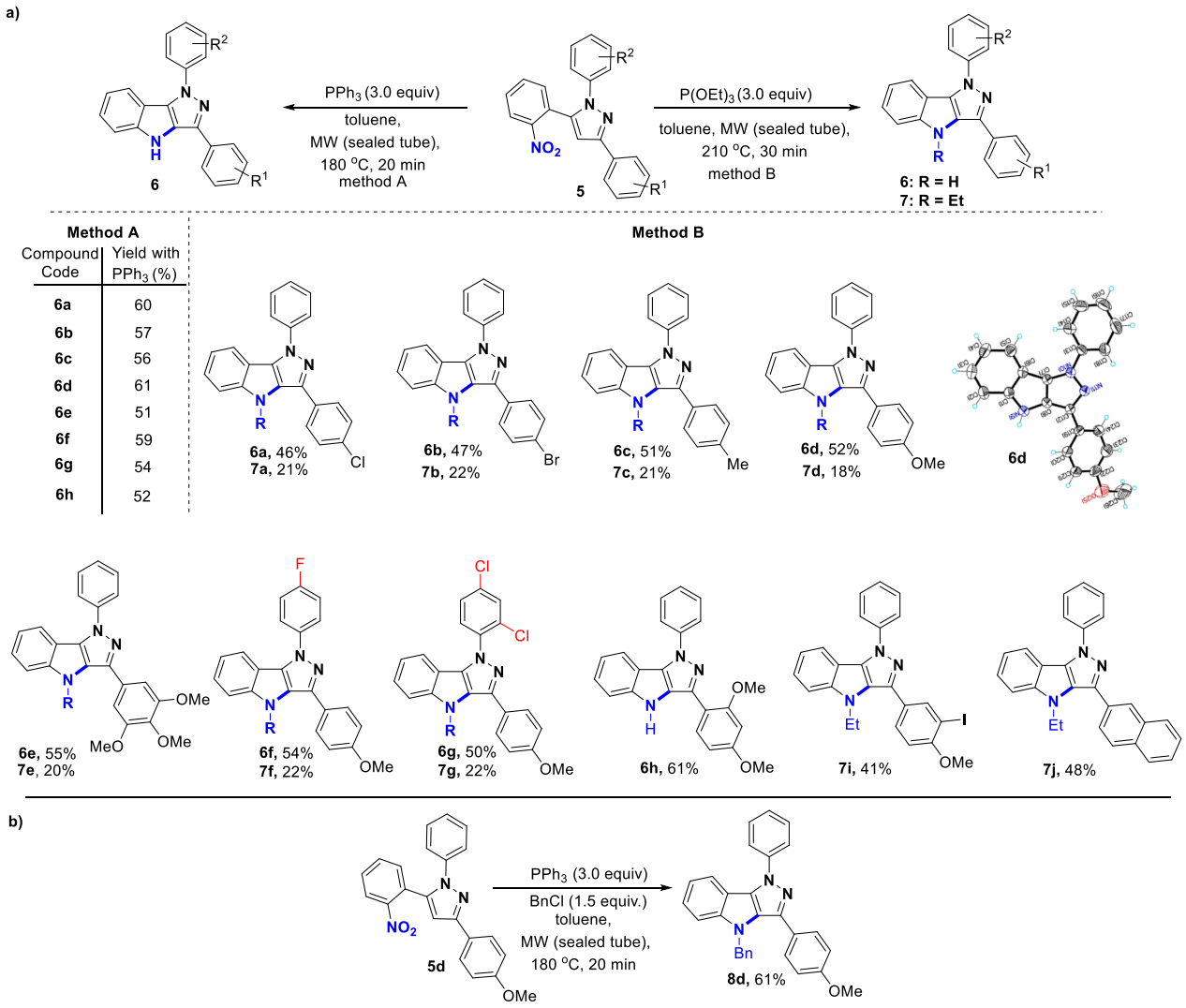

Scheme 2. **a** and **b**. Synthesis of target compounds.

2.2. Biology

2.2.1. Evaluation of anticancer activity, alteration in mitochondrial membrane potential and redox parameter, and topoisomerase inhibition by the target compounds

All the target compounds were tested for cytotoxicity potential against A549 (lung), HCT-116 (colon), and MDA-MB-231 (breast), and MCF-7 (breast) cancer cell lines. All the compounds showed good anti-proliferative activities (Table 2) with IC_{50} values in the low micromolar range. The results were then represented from three independent experiments with the absorbance of the formazan formed in control (media only) cells taken as 100% viability, and the results of the MTT assay were plotted in graphical form (Fig. 5). Camptothecin (CPT) and etoposide were taken as reference drugs. Three different concentrations (1 μM, 5 μM, 25 μM) of the compounds were used, and treatments were given for 24 h. Although all the tested compounds exhibited low μM IC_{50s}, **7a**, **7b**, and **6h** emerged as broad-spectrum antiproliferative compounds (IC_{50} range 0.58−2.41 μM; Table 2 and Fig. 5) comparable to standard drugs. Further, to determine the toxicity of these lead compounds on normal cells, we isolated human peripheral blood mononuclear cells (hPBMCs), and an MTT assay was performed. The results did not show any significant toxicity towards hPBMC tested at 10 and 25 μM concentration of the compounds for 48 h (Figure S2). After that, compounds were examined further for their various other impacts on cancer cells.

Compounds **6h**, **7a**, and **7b** were tested for Topo I mediated DNA relaxation assay to assess Topo I inhibitory potential. The results for Topo I inhibition assay showed that these chosen compounds exerted Topo I inhibitory activity. In the presence of Topo I inhibitor, the enzyme is unable to remove the supercoils. The inhibition of relaxation was measured by densitometry showing that compound **6h** showed better Topo I inhibition compared to camptothecin (Fig. 6A; Lane 7). **7a** (Lane 5) and **7b** (Lane 6) also displayed inhibition of Topo I mediated relaxation of supercoiled DNA though they were less effective than camptothecin (Fig. 6B).

Furthermore, for the Topo II inhibition assay, kDNA was used as a substrate for Topo II. Gel image shows that in the presence of Topo II, kDNA gets decatenated. However, in the presence of a Topo II inhibitor like etoposide, the decatenation gets reduced (Fig. 6 C; Lane 3). Interestingly, compounds **7a** and **7b** emerged as better Topo II inhibitors than etoposide. In contrast to these, compound **6h** (Lane 6) displayed weak Topo II inhibitory activity, and thus, we deduce that compound **7a** (Lane 4) and **7b** (Lane 5) are strong Topo II inhibitors (Fig. 6 D). Furthermore, topoisomerase binding assays revealed that **6h** inhibited Topo I, whereas **7a** and **7b** inhibited Topo II to a greater extent than the standard drugs.

This observation was further supported by *in silico* studies (Figure S3), which revealed some critical interactions (Fig. 6E and F), such as when **7a** docked at the Topo I binding site, it intercalates with

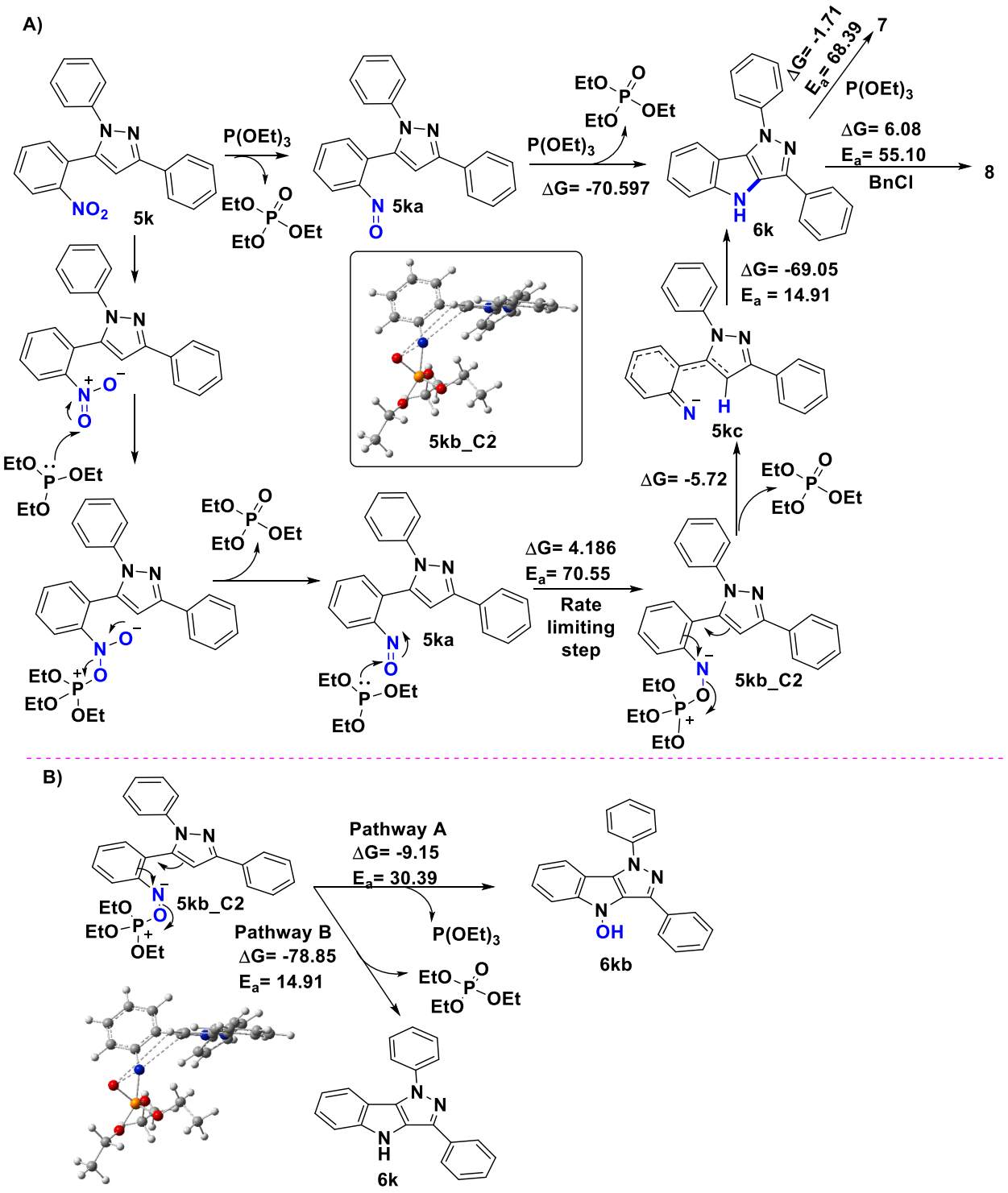

Fig. 3. A plausible mechanism of the reaction.

DNA and interacts with DG-12, DC-111, DC-112 residues. In addition, pyrazole ring nitrogen of **7a** showed hydrogen bonding with ARG364, and the aromatic hydrogens of two phenyl rings showed weak hydrogen bonding with ASP533. Furthermore, the docking of **7a** into Topo II disclosed that chlorine substituted phenyl ring displayed π-cation interactions with ARG98, weak hydrogen bonding with SER149. Interestingly, the 1,4-dihydropyrazolo[4,3-*b*]indole nucleus interacted with conserved Walker A motif lined by ARG162, ASN163, GLY164, TYR165, GLY166 and ALA167, responsible for Topo II inhibition.

Further, the tested compounds were investigated for their ability to alter mitochondrial membrane potential (MMP) and ROS level in MDA-MB-231 cells. Interestingly, the studies revealed that these compounds modulated the MMP as indicated by an increase in the Red Green ratio leading to hyperpolarization of the membrane, as shown in Fig. 7.

Additionally, the intracellular ROS was measured by treating the washed cells with H2DCFDA (2′, 7′–dichlorofluorescein diacetate) for 30 min at 37C and then analyzed using a flow cytometer. This investigation revealed that compounds **7a**, **7b**, and **6h** induced oxidative stress, as evidenced by an upsurge in ROS generation compared to the control (Fig. 8).

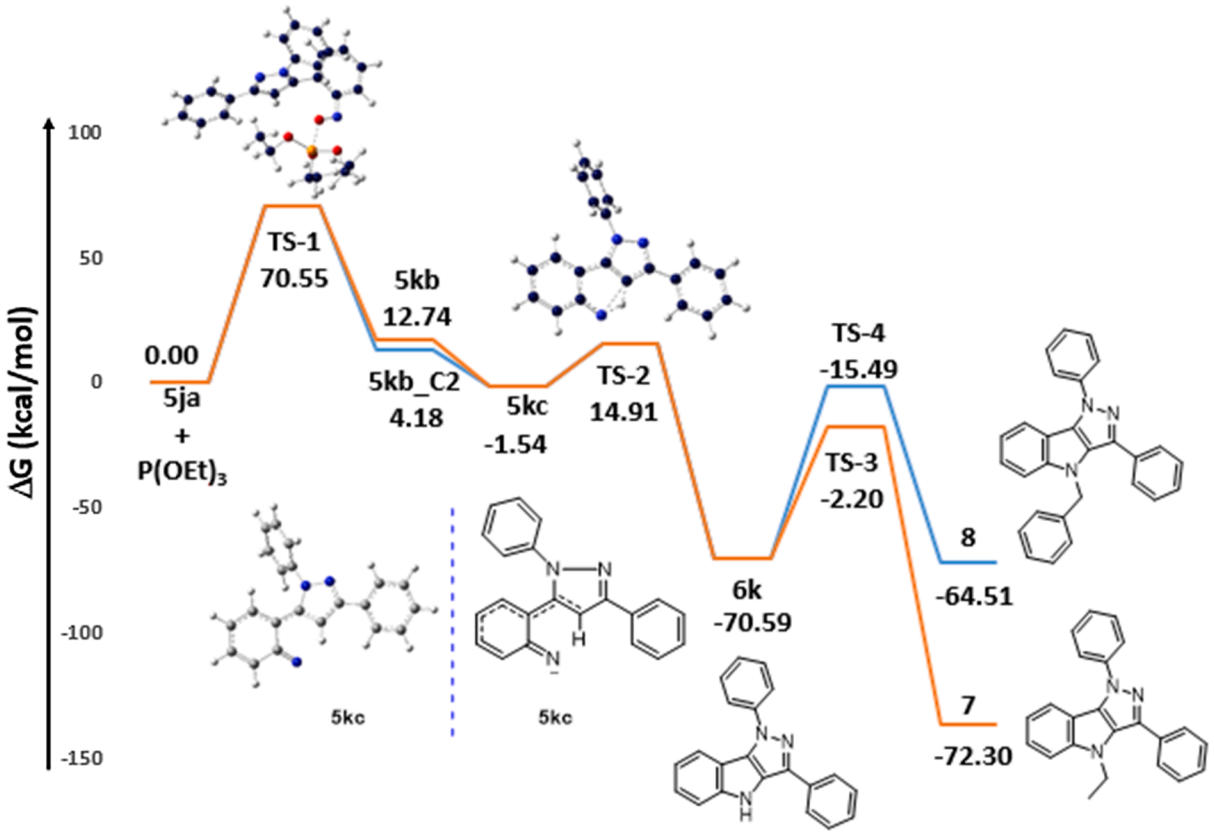

Fig. 4. Potential Energy Surface Diagram representing the cyclization process via nitrene pathway.

Therefore, from the biological evaluation, the investigation provided significant findings in the context of the anti-cancer potential of the synthesized compounds. Interestingly, all the compounds exhibited antiproliferative activity at a low micro-molar range, among which **6h**, **7a** and **7b** were the most effective compounds. The further elucidation of the anticancer mechanism revealed that **6h** inhibited topoisomerase I while **7a** and **7b** were potent topoisomerase II inhibitors. It is found from the literature that the cancer cells usually have fine-tuned ROS homeostasis, which allows them to operate pro-tumorigenic signaling without undergoing ROS induced cell death[45], and the cancer treatments like chemotherapy rely on generating ROS levels which activate intrinsic apoptosis[46]. Thus, to know about the mechanism of cell death, the compounds were further investigated, and it was found that our compounds were also able to induce cell death via ROS burst and hyperpolarisation of the mitochondrial membrane.

3. Conclusions

To encapsulate, we have described a new synthetic protocol for the construction of undocumented 1,4-dihydropyrazolo[4,3-*b*]indoles involving intramolecular C(sp^2)-N bond formation under modified Cadogan reaction. DFT calculations rationalized the formation of products via the nitrene mechanism. The biological studies revealed that **7a, 7b,** and **6h** were cytotoxic towards cancer cells, induced ROS generation and altered the mitochondrial membrane potential of highly aggressive MDA-MB-231 cells. Further investigations revealed that these compounds were selective Topo I (**6h)** or Topo II (**7a, 7b**) inhibitors. Thus, the work offers the opportunity to synthesize products with substitution at N-1, C-3 and N-4 positions of 1,4-dihydropyrazolo[4,3-*b*] indoles required for further structure–activity relationship (SAR) study for pharmaceuticals as well as supramolecular chemistry perspective.

4. Experimental section

4.1. Chemistry

General Methods and Materials. Biotage® Initiator microwave synthesizer (Company: Biotage® Model No. 355,301 (Initiator EXPEU)) (used for sealed reactions) and Discover System; Company: CEM; Model No. 908010; Serial No. DU9671) (used for open reflux reactions) were used for carrying out microwave reactions at 200 W power. ^{1}H NMR and ^{13}C NMR spectra were obtained in $CDCl_3$/d_6-DMSO on 400/500 MHz and 100/125 MHz Bruker Advance II NMR spectrometer/Jeol, respectively TMS ($\delta = 0$) as an internal standard. Data were reported as follows: Chemical shifts (δ) are reported in ppm, coupling constants (*J*) are in Hertz (Hz). Abbreviations used to explain the multiplicities: s = singlet, d = doublet, t = triplet, q = quartet, m = multiplet. Column chromatography was performed with silica gel (60–120 and 100–200 mesh ASTM) to purify compounds. Melting points were measured with a melting point instrument and were uncorrected.

All the reagents were purchased from commercial suppliers and used without further purification. Reactions were monitored by TLC (detection with UV light).

General procedure for the synthesis of nitro precursors. (a) To a methanol solution containing acetophenones **1** (1.0 equiv) and 2-nitrobenzaldehyde **2** (1 equiv) was added NaOH (10%). The reaction mixture was stirred at room temperature for 2–3 h. After the completion of the reaction (TLC), the reaction mixture was poured into the water and filtered. The solid compounds (**3**) were washed with methanol and dried.

Analytical data of reference compound, 3a (precursor of 4a). (*E*)-1-(4-chlorophenyl)-3-(2-nitrophenyl)prop-2-en-1-one (**3a**). Cream yellow solid; 75% yield; ^{1}H NMR (500 MHz, DMSO-d_6): δ 8.22 (d, J = 7.8 Hz, 1H), 8.13 – 8.12 (m, 3H), 8.04 – 8.00 (m, 1H), 7.92 – 7.82 (m, 4H), 7.75–7.72 (m, 1H); ^{13}C NMR (125 MHz, DMSO-d_6) δ 188.75,

Table 2
IC_{50} values of synthesized compounds against various cancer cell lines.

Antiproliferative potential IC_{50} (μM)[a]				
Compound Code	**MDA-MB-231 (Breast)**	**MCF7 (Breast)**	**A549 (Lung)**	**HCT116 (Colon)**
6a	2.55 ± 0.21	2.6 ± 0.12	3.35 ± 0.32	2.8 ± 0.26
6b	3.22 ± 0.11	2.97 ± 0.32	2.84 ± 0.47	1.84 ± 0.1
6c	3.41 ± 0.51	2.65 ± 0.24	2.3 ± 0.29	2.7 ± 0.36
6d	2.3 ± 0.23	3.39 ± 0.18	2.78 ± 0.42	3.01 ± 0.3
6e	2.84 ± 0.27	2.6 ± 0.13	3.56 ± 0.3	2.87 ± 0.36
6f	2.34 ± 0.74	3.1 ± 0.69	4.72 ± 0.37	6.47 ± 0.11
6g	3.53 ± 0.42	2.89 ± 0.31	4.67 ± 0.59	4.14 ± 0.4
6h	1.58 ± 0.56	1.69 ± 0.26	1.87 ± 0.47	1.69 ± 0.2
7a	0.99 ± 0.24	1.29 ± 0.28	1.21 ± 0.50	1.47 ± 0.42
7b	0.84 ± 0.19	0.58 ± 0.13	1.63 ± 0.24	2.41 ± 0.44
7c	2.38 ± 0.21	3.28 ± 0.47	3.43 ± 0.51	2.99 ± 0.11
7d	2.49 ± 0.25	3.35 ± 0.41	3.24 ± 0.31	3.01 ± 0.27
7e	1.51 ± 0.29	2.53 ± 0.38	2.24 ± 0.45	3.01 ± 0.21
7f	2.34 ± 0.15	2.78 ± 0.36	3.24 ± 0.29	2.97 ± 0.39
7g	3.01 ± 0.14	2.84 ± 0.47	2.24 ± 0.16	3.03 ± 0.19
7i	2.43 ± 0.41	3.1 ± 0.24	3.28 ± 0.21	2.62 ± 0.17
7j	3.1 ± 0.1	3.25 ± 0.46	7.46 ± 0.16	3.76 ± 0.26
8d	3.22 ± 0.62	2.49 ± 0.23	3.41 ± 0.21	3.1 ± 0.32
Etoposide	2.05 ± 0.33	3.47 ± 0.41	3.14 ± 0.29	3.58 ± 0.28
Camptothecin (CPT)	0.21 ± 0.11	0.97 ± 0.27	1.65 ± 0.37	0.95 ± 0.3

[a] Data was represented as mean ± S.E. from three independent experiments.; Camptothecin and Etoposide were taken as positive controls.

149.30, 139.51, 136.54, 134.27, 132.45, 131.68, 131.23, 130.14, 130.04, 128.24, 126.56, 125.23; MS (ESI): $m/z = 287.7$

(b) Further, **3** (1 mmol) were mixed with various substituted phenyl hydrazines (2–3 mmol) in methanol and refluxed for 3 h. The reaction was monitored by TLC, and the solvent was evaporated under vacuum to get **4**.

Analytical data of reference compound, 4a (precursor of 5a). 3-(4-chlorophenyl)-5-(2-nitrophenyl)-1-phenyl-4,5-dihydro-1H-pyrazole (**4a**)**.** Peach solid; 93% yield; ^{1}H NMR (500 MHz, DMSO-d_6): δ 8.16 (d, J = 8.1 Hz, 1H), 7.77 (d, J = 8.5 Hz, 2H), 7.66 (t, J = 7.6 Hz, 1H), 7.56 (t, J = 7.7 Hz, 1H), 7.50 (m, 2H), 7.26 (t, J = 11.2 Hz, 1H), 7.18 (t, J = 7.9 Hz, 2H), 6.96 (d, J = 8.1 Hz, 2H), 6.76 (t, J = 7.3 Hz, 1H), 5.95–5.91 (m, 1H), 4.08 (m, 1H), 3.32 – 3.29 (m, 1H); ^{13}C NMR (125 MHz, DMSO-d_6) δ 147.85, 147.12, 143.87, 136.72, 134.94, 133.79, 131.42, 129.57, 129.53, 129.18, 128.08, 127.96, 125.93, 119.60, 113.21, 60.53, 42.82; MS (ESI): $m/z = 377.8$

(c) Catalytic amount of molecular iodine was added to **4** in DMSO and refluxed for 4 h. TLC was done for reaction confirmation. The mixture was poured in ice cold water and ethyl acetate was used for extraction of **5**. The organic layer was washed with sodium thiosulphate solution, so that the traces of iodine get removed. Then the organic layer was filtered *via* drying it over sodium sulphate. The filtrate was evaporated under vacuum to get **5**.

Analytical data of representative nitro substrate, 5a (precursors of 6a). 3-(4-chlorophenyl)-5-(2-nitrophenyl)-1-phenyl-1H-pyrazole (**5a**). Yellow solid; 89% yield; ^{1}H NMR (400 MHz, DMSO-d_6): δ 8.07 (d, J = 8.1 Hz, 1H), 7.97 (d, J = 8.5 Hz, 2H), 7.84 (t, J = 7.5 Hz, 1H), 7.74 (t, J = 7.3 Hz, 1H), 7.69 (d, J = 7.5 Hz, 1H), 7.54 (d, J = 8.5 Hz, 2H), 7.40–7.33 (m, 3H), 7.26 (d, J = 7.2 Hz, 2H), 7.20 (s, 1H), ^{13}C NMR (100 MHz, DMSO-d_6): δ 150.40, 148.63, 140.12, 139.23, 134.36, 133.31, 133.18, 131.75, 131.42, 129.66, 129.36, 128.28, 127.57, 125.23, 125.11, 124.56, 106.65; MS (ESI): $m/z = 375.8$

General Procedure for the synthesis of 1,4-Dihydropyrazolo [4,3-*b*] indoles (6 and **7).** To an oven-dried Microwave vial was added pyrazole-based nitro compound **5** (1 mmol, 1 equiv), PPh_3/$P(OEt)_3$ (3 equiv), and toluene (5 mL). The mixture was stirred at 180/210 °C (method A and B) in the CEM (sealed tube). After TLC indicated that **5** was consumed entirely, toluene was evaporated under vacuum, and the mixture was poured in water and extracted with ethyl acetate (25 mL). Then the solvent was evaporated under vacuum. Finally, the crude products were purified using flash column chromatography (eluent: Petroleum ether/Acetone) on silica gel to afford the desired products **6** and **7**.

Analytical data of products (**6** and **7**)

3-(4-chlorophenyl)-1-phenyl-1,4-dihydropyrazolo[4,3-*b*]indole (**6a**)

Compound **6a** was synthesized in accordance with the typical procedure discussed above. Purification by column chromatography on silica gel (PE/A = 19:1) afforded **6a** (60%) as a cream solid; mp: 191–193 °C; ^{1}H NMR (400 MHz, DMSO-d_6): δ 11.58 (s, 1H), 8.09 (d, J = 8.5 Hz, 2H), 7.91 (d, J = 7.8 Hz, 2H), 7.85 (d, J = 8.0 Hz, 1H), 7.65 – 7.53 (m, 5H), 7.40–7.33 (m, 2H), 7.13 (t, J = 7.5 Hz, 1H). ^{13}C NMR (100 MHz, DMSO-d_6): δ 144.98, 140.76, 132.93, 132.67, 132.12, 131.54, 130.36, 130.26, 129.51, 127.73, 126.88, 125.35, 120.80, 119.51, 119.50, 113.70, 112.75; HRMS: for $C_{21}H_{14}ClN_3$, Exact mass: 343.0876; observed $[M + H]^+$: 344.0952.

3-(4-bromophenyl)-1-phenyl-1,4-dihydropyrazolo[4,3-*b*]indole (**6b**)

Compound **6b** was synthesized in accordance with the typical procedure discussed above. Purification by column chromatography on silica gel (PE/A = 19:1) afforded **6b** (57%) as a yellow white solid; mp: 212–214 °C; ^{1}H NMR (400 MHz, DMSO-d_6): δ 11.58 (s, 1H), 8.02 (d, J = 8.5 Hz, 2H), 7.91 (d, J = 7.8 Hz, 2H), 7.85 (d, J = 8.0 Hz, 1H), 7.71 (d, J = 8.4 Hz, 2H), 7.63 (t, J = 7.8 Hz, 2H), 7.54 (d, J = 8.3 Hz, 1H), 7.40–7.33 (m, 2H), 7.13 (t, J = 7.5 Hz, 1H); ^{13}C NMR (100 MHz, DMSO-d_6): δ 144.97, 140.73, 132.97, 132.39, 132.14, 131.86, 130.36, 130.24, 128.00, 126.91, 125.37, 121.23, 120.80, 119.54, 119.48, 113.70, 112.73; HRMS: for $C_{21}H_{14}BrN_3$, Exact mass: 387.0371; observed $[M + H]^+$: 388.0436.

1-phenyl-3-(p-tolyl)-1,4-dihydropyrazolo[4,3-*b*]indole (**6c**)

Compound **6c** was synthesized in accordance with the typical procedure discussed above. Purification by column chromatography on silica gel (PE/A = 19:1) afforded **6c** (56%) as a light yellow solid; mp: 218–220 °C; ^{1}H NMR (400 MHz, DMSO-d_6): δ 11.50 (s, 1H), 7.97 (d, J = 8.1 Hz, 2H), 7.90 (d, J = 7.9 Hz, 2H), 7.85 (d, J = 8.0 Hz, 1H), 7.62 (t, J = 7.9 Hz, 2H), 7.54 (d, J = 8.3 Hz, 1H), 7.31–7.38 (m, 4H), 7.12 (t, J = 7.5 Hz, 1H), 2.35 (s, 3H); ^{13}C NMR (100 MHz, DMSO-d_6): δ 144.92, 140.92, 137.66, 134.22, 131.84, 130.31, 130.03, 129.85, 126.55, 126.04, 125.13, 122.50, 120.61, 119.45, 119.37, 113.68, 112.81, 21.46; HRMS: for $C_{22}H_{17}N_3$, Exact Mass: 323.1422; observed $[M + H]^+$: 324.1485.

3-(4-methoxyphenyl)-1-phenyl-1,4-dihydropyrazolo[4,3-*b*]indole (**6d**)

Compound **6d** was synthesized in accordance with the typical procedure discussed above. Purification by column chromatography on silica gel (PE/A = 19:1) afforded **6d** (61%) as a cream solid; mp: 221–223 °C; ^{1}H NMR (400 MHz, DMSO-d_6): δ 11.48 (s, 1H), 8.00 (d, J = 8.6 Hz, 2H), 7.90–7.84 (m, 3H), 7.61 (t, J = 7.0 Hz, 2H), 7.53 (d, J = 8.4 Hz, 1H), 7.37–7.31 (m, 2H), 7.14 – 7.06 (m, 3H), 3.81 (s, 3H); ^{13}C NMR (100 MHz, DMSO-d_6): δ 159.53, 144.91, 140.96, 134.16, 131.79, 130.30, 130.11, 127.51, 126.41, 125.22, 125.09, 120.52, 119.47, 119.33, 114.89, 113.67, 112.85, 55.77; HRMS: for $C_{22}H_{17}N_3O$, Exact Mass: 339.1372; observed $[M + H]^+$: 340.1452.

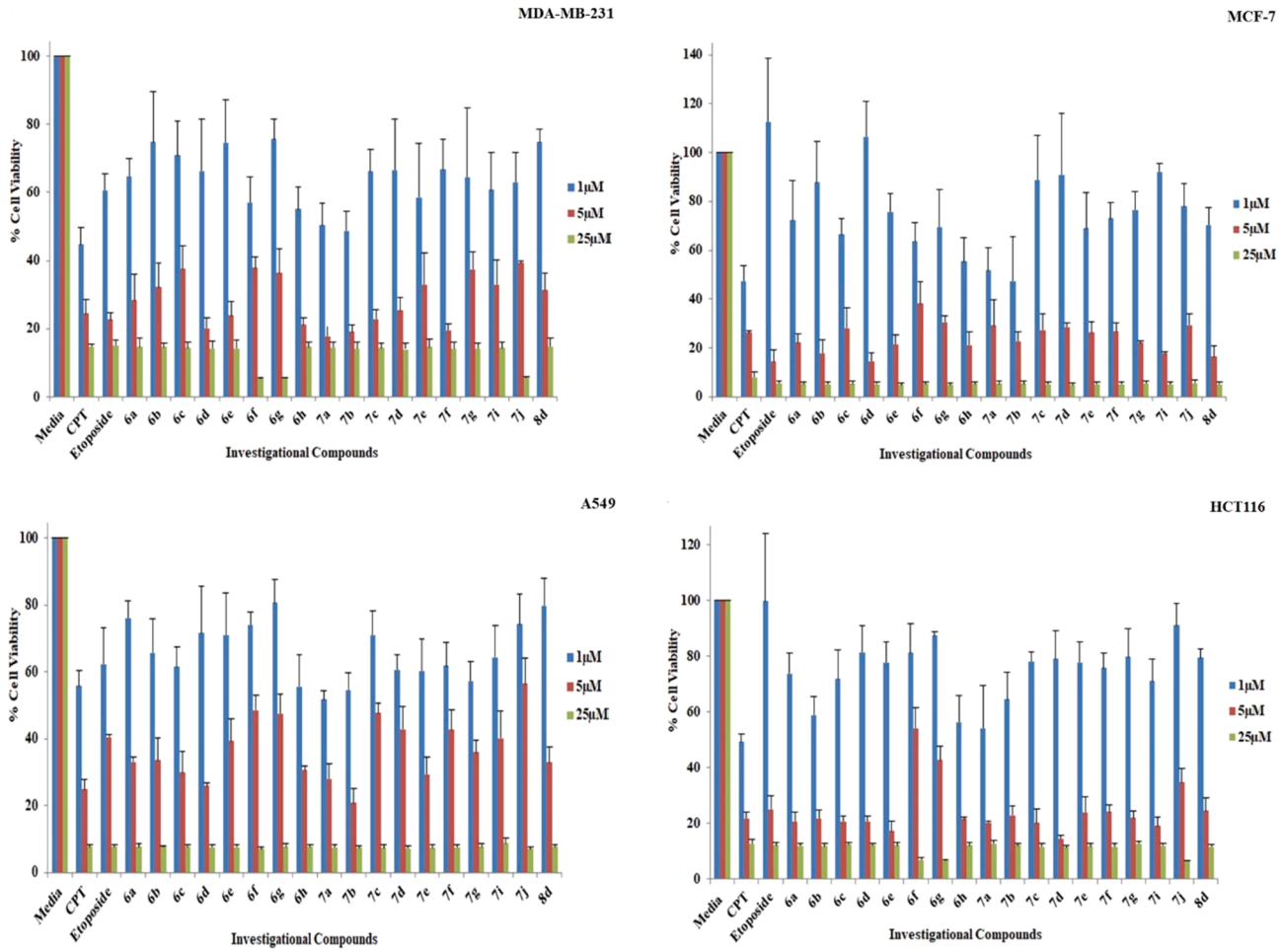

Fig. 5. *In vitro* evaluation of the antiproliferative potential of the indicated compounds in different cell lines at indicated concentrations after 24 h of treatment. Camptothecin (CPT) and etoposide were used as positive controls.

1-phenyl-3-(3,4,5-trimethoxyphenyl)-1,4-dihydropyrazolo[4,3-*b*] indole (**6e**)

Compound **6e** was synthesized in accordance with the typical procedure discussed above. Purification by column chromatography on silica gel (PE/A = 19:1) afforded **6e** (51%) as a cream solid; mp: 225–227 °C; ^{1}H NMR (400 MHz, DMSO-d_6): δ 11.5 (s, 1H), 7.9 (m, 3H), 7.7 (m, 2H), 7.6 (m, 1H), 7.4 (m, 2H), 7.3 (m, 2H), 7.2 (m, 1H), 4 (s, 6H), 3.8 (s, 3H). ^{13}C NMR (100 MHz, DMSO-d_6): δ 153.96, 145.01, 140.84, 139.01, 137.99, 134.23, 132.08, 130.32, 128.37, 126.70, 125.25, 122.67, 120.81, 119.46, 113.67, 112.95, 103.77, 60.70, 56.76; HRMS: for $C_{24}H_{21}N_3O_3$, Exact Mass: 399.1583; observed $[M + H]^+$: 400.1670.

1-(4-fluorophenyl)-3-(4-methoxyphenyl)-1,4-dihydropyrazolo[4,3-*b*]indole (**6f**)

Compound **6f** was synthesized in accordance with the typical procedure discussed above. Purification by column chromatography on silica gel (PE/A = 19:1) afforded **6f** (59%) as a light yellowish solid; mp: 175–176 °C; ^{1}H NMR (400 MHz, DMSO-d_6) δ 11.44 (s, 1H), 7.99 (d, J = 8.3 Hz, 2H), 7.92–7.89 (m, 2H), 7.81 (d, J = 8.0 Hz, 1H), 7.53 (d, J = 8.3 Hz, 1H), 7.45 (t, J = 8.7 Hz, 2H), 7.35–7.31 (m, 1H), 7.13 – 7.06 (m, 3H), 3.81 (s, 3H). ^{13}C NMR (100 MHz, DMSO- d$_6$) δ 159.54, 144.91, 137.52, 134.18, 131.88, 130.04, 127.51, 125.12, 122.55, 122.47, 119.35, 119.31, 117.21, 116.98, 114.88, 113.67, 112.71, 55.77; HRMS: for $C_{22}H_{16}FN_3O$, Exact Mass: 357.1277; observed $[M + H]^+$: 358.1371.

1-(2,4-dichlorophenyl)-3-(4-methoxyphenyl)-1,4-dihydropyrazolo [4,3-*b*]indole (**6g**)

Compound **6 g** was synthesized in accordance with the typical procedure discussed above. Purification by column chromatography on silica gel (PE/A = 19:1) afforded **6 g** (54%) as a yellow solid; mp: 177–178 °C; ^{1}H NMR (400 MHz, DMSO-d_6): δ 11.42 (s, 1H), 7.98–7-75 (m, 3H), 7.74 – 7.63 (m, 2H), 7.49 (d, J = 8.3 Hz, 1H), 7.34 – 7.26 (m, 2H), 7.07 – 7.0 (m, 3H), 3.80 (s, 3H). ^{13}C NMR (100 MHz, DMSO-d_6) δ 159.60, 144.76, 137.53, 134.80, 134.51, 133.79, 130.77, 130.21, 129.18, 129.00, 127.58, 125.10, 125.02, 119.27, 119.18, 114.88, 113.47, 112.93, 55.77; HRMS: for $C_{22}H_{15}Cl_2N_3O$, Exact Mass: 407.0592; observed $[M + H]^+$: 408.0662

3-(2,4-dimethoxyphenyl)-1-phenyl-1,4-dihydropyrazolo[4,3-*b*] indole (**6h**)

Compound **6 h** was synthesized in accordance with the typical procedure discussed above. Purification by column chromatography on silica gel (PE/A = 19:1) afforded **6 h** (52%) as a light yellowish solid; mp: 158–160 °C; ^{1}H NMR (400 MHz, DMSO-d_6): δ 10.35 (s, 1H), 7.88 (d, J = 7.9 Hz, 2H), 7.82 (d, J = 8.5 Hz, 2H), 7.62–7.56 (m, 3H), 7.36–7.27 (m, 2H), 7.07 (t, J = 7.6 Hz, 1H), 6.72 (d, J = 2.2 Hz, 1H), 6.66–6.63 (m, 1H), 3.94 (s, 3H), 3.81 (s, 3H). ^{13}C NMR (100 MHz, DMSO-d_6): δ 161.31, 158.08, 144.06, 140.96, 132.14, 131.68, 130.84, 130.25, 129.90, 126.29, 124.71, 120.68, 119.22, 118.82, 114.26, 113.78, 112.50, 106.18, 99.05, 56.66, 55.90; HRMS: for $C_{23}H_{19}N_3O_2$, Exact Mass: 369.1477; observed $[M + H]^+$: 370.1558.

3-(4-chlorophenyl)-4-ethyl-1-phenyl-1,4-dihydropyrazolo[4,3-*b*] indole (**7a**)

Compound **7a** was synthesized in accordance with the typical procedure discussed above. Purification by column chromatography on silica gel (PE/A = 99:1) afforded **7a** (21%) as a cream solid; mp: 170–172 °C; ^{1}H NMR (400 MHz, DMSO-d_6): δ 7.89 – 7.81 (m, 5H), 7.67 –

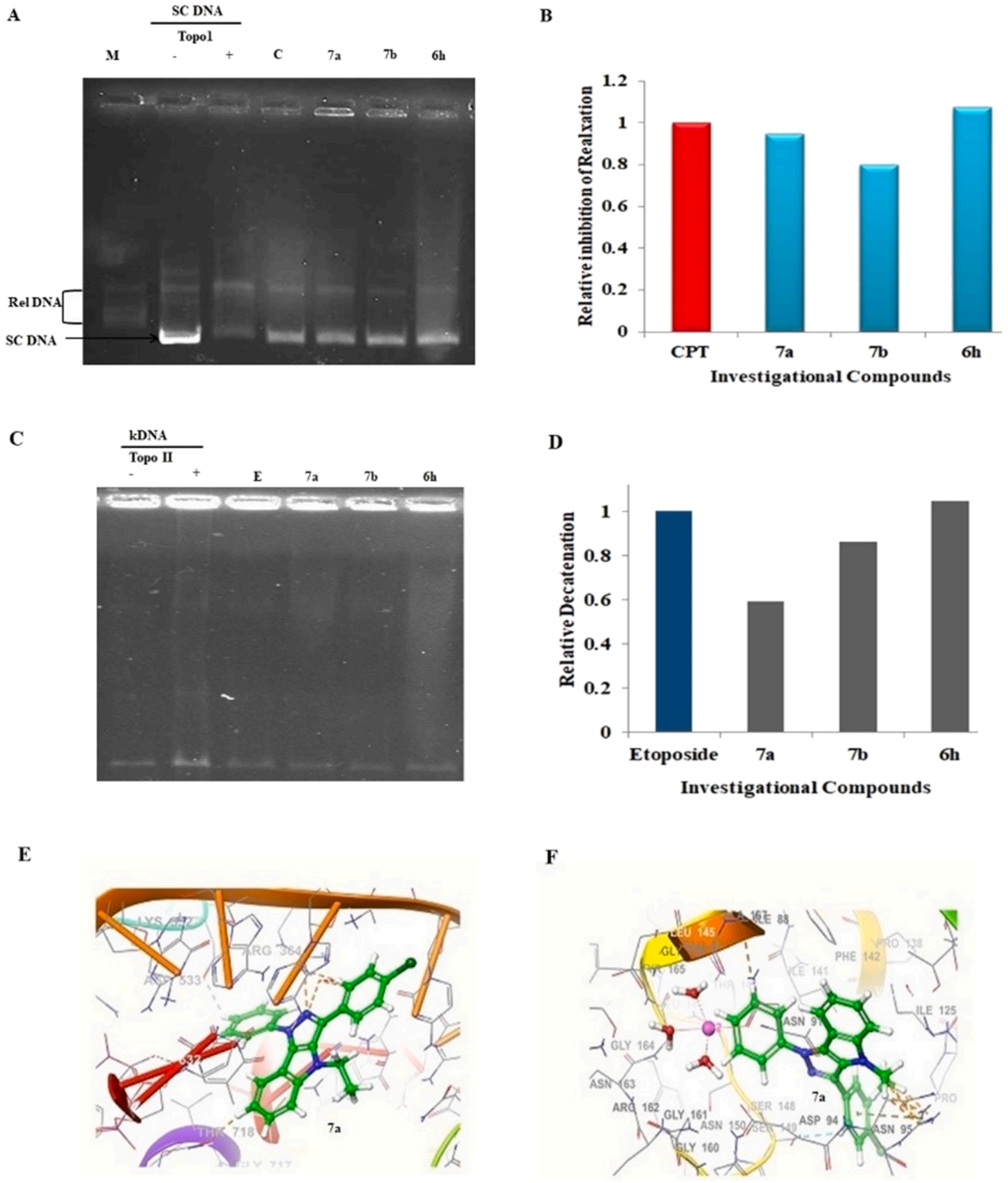

Fig. 6. **A**. Agarose gel image depicting the inhibition of Topo I activity **B**. Graph showing relative inhibition of relaxation of supercoiled DNA by compounds (100 μM). M: Marker; C: CPT. **C**. Gel image showing decatenation of kDNA when treated with Topo II and its inhibition by compounds (100 μM). **D.** Quantification of relative decatenation showing Topo II inhibition. **E.** Binding pose of **7a** with Topo I and **F.** Topo II active site residues.

7.58 (m, 5H), 7.39 (t, $J = 7.7$ Hz, 2H), 7.14 (t, $J = 7.5$ Hz, 1H), 4.33 (q, $J = 7.0$ Hz, 2H), 1.07 (t, $J = 7.1$ Hz, 3H); ^{13}C NMR (100 MHz, DMSO-d_6): δ 144.32, 140.58, 134.24, 133.38, 131.91, 131.53, 131.06, 130.49, 130.35, 129.38, 127.11, 125.46, 121.15, 119.61, 119.42, 112.60, 111.78, 40.61, 14.98; HRMS: for $C_{23}H_{18}ClN_3$, Exact Mass: 371.1189; observed $[M + H]^+$: 372.1277.

3-(4-bromophenyl)-4-ethyl-1-phenyl-1,4-dihydropyrazolo[4,3-*b*] indole (**7b**)

Compound **7b** was synthesized in accordance with the typical procedure discussed above. Purification by column chromatography on silica gel (PE/A = 99:1) afforded **7b** (22%) as a cream solid; mp: 174–176 °C; ^{1}H NMR (400 MHz, DMSO-d_6): δ 7.89–7.606 (m, 10*H*), 7.39–7.37 (m, 2H), 7.16–7.11 (m, 1H), 4.308 (m, 2H), 1.07 (m, 3H); ^{13}C NMR (100 MHz, DMSO-d_6): δ 144.45, 140.58, 134.28, 132.29, 131.57, 31.03, 130.77, 130.35, 127.12, 125.48, 122.00, 121.16, 119.61, 119.43, 112.60, 111.79, 40.20, 14.98; HRMS: for $C_{23}H_{18}BrN_3$, Exact Mass:

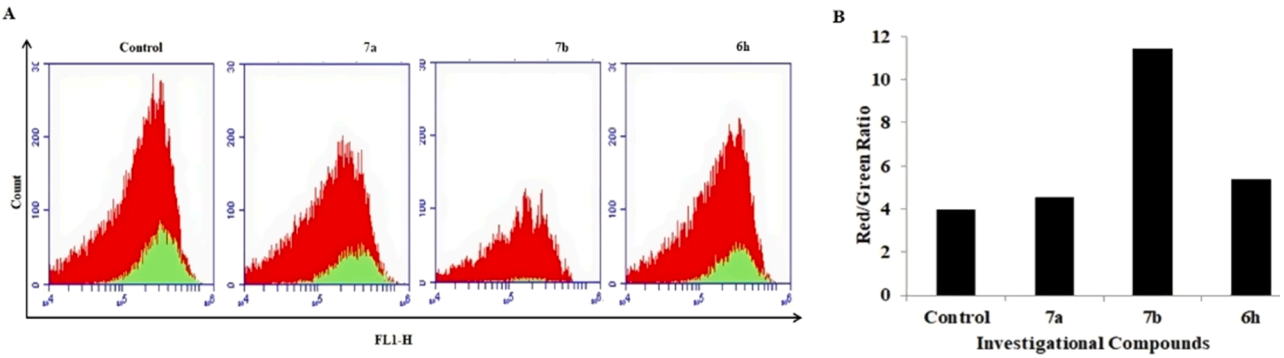

Fig. 7. A. Measurement of alteration of Mitochondrial Membrane Potential by flow cytometer. **B**. Ratiometric values showing the alteration in the ratio of Red (J-aggregates) to green (J-Monomer) fluorescence intensity.

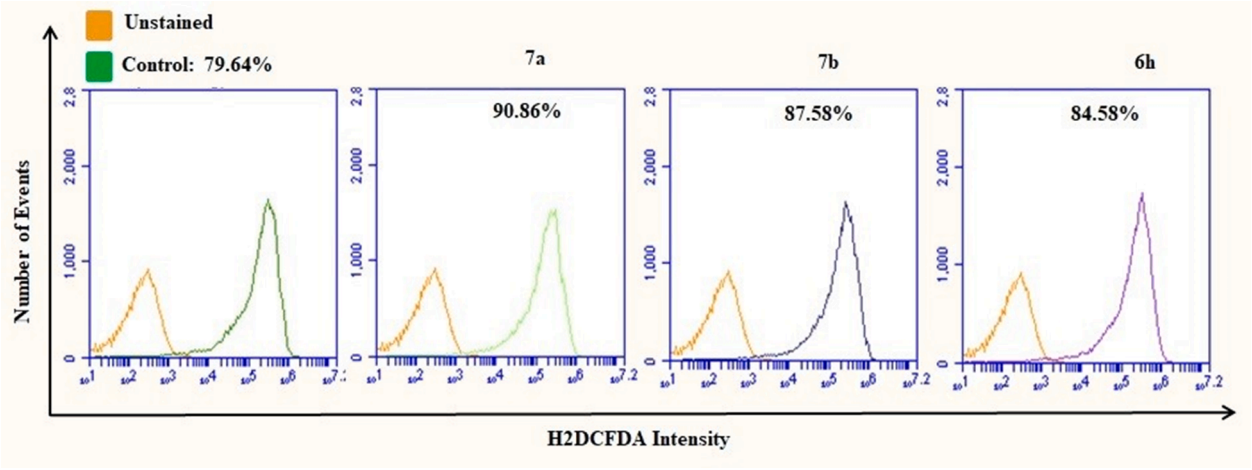

Fig. 8. Measurement of ROS alteration by flow cytometry. Compared to control, all the selected compounds could enhance ROS production at IC_{50} values in MDA-MB-231 cells.

415.0684; observed $[M + H]^+$: 416.0760.

4-ethyl-1-phenyl-3-(p-tolyl)-1,4-dihydropyrazolo[4,3-*b*]indole (**7c**)

Compound **7c** was synthesized in accordance with the typical procedure discussed above. Purification by column chromatography on silica gel (PE/A = 99:1) afforded **7c** (21%) as a cream solid; mp: 171–173 °C; ^{1}H NMR (400 MHz, DMSO-d_6): δ 7.88–7.83 (m, 3H), 7.69 – 7.59 (m, 5H), 7.39 – 7.32 (m, 4H), 7.13 (t, J = 7.5 Hz, 1H), 4.35–4.30 (m, 2H), 2.37 (s, 3H)1.06 (t, J = 7.0 Hz, 3H); ^{13}C NMR (100 MHz, DMSO-d_6): δ 144.22, 140.73, 138.05, 135.57, 131.25, 131.19, 130.31, 130.14, 129.87, 128.72, 126.83, 125.28, 120.99, 119.60, 119.29, 112.69, 111.75, 40.63, 21.44, 14.99; HRMS: for $C_{24}H_{21}N_3$, Exact Mass: 351.1735; observed $[M + H]^+$: 352.1831.

4-ethyl-3-(4-methoxyphenyl)-1-phenyl-1,4-dihydropyrazolo[4,3-*b*] indole (**7d**)

Compound **7d** was synthesized in accordance with the typical procedure discussed above. Purification by column chromatography on silica gel (PE/A = 99:1) afforded **7d** (18%) as a cream solid; mp: 152–154 °C; ^{1}H NMR (400 MHz, DMSO-d_6): δ 7.88 – 7.83 (m, 3H), 7.74 – 7.70 (m, 2H), 7.64–7.59 (m, 3H), 7.40–7.35 (m, 2H), 7.15 – 7.07 (m, 3H), 4.35–4.30 (m, 2H), 3.81 (s, 3H), 1.07 (t, J = 7.1 Hz, 3H); ^{13}C NMR (100 MHz, DMSO-d_6): δ 159.76, 144.18, 140.76, 135.43, 131.16, 130.30, 130.12, 126.73, 125.31, 125.24, 120.91, 119.61, 119.26, 114.70, 112.70, 111.72, 55.73, 40.67, 15.01; HRMS: for $C_{24}H_{21}N_3O$, Exact Mass: 367.1685; observed $[M + H]^+$: 368.1761.

4-ethyl-1-phenyl-3-(3,4,5-trimethoxyphenyl)-1,4-dihydropyrazolo [4,3-*b*]indole (**7e**)

Compound **7e** was synthesized in accordance with the typical procedure discussed above. Purification by column chromatography on silica gel (PE/A = 99:1) afforded **7e** (20%) as a cream yellow; mp: 138–140 °C; ^{1}H NMR (400 MHz, DMSO-d_6): δ 8 (d, J = 8.7 Hz, 1H), 7.93–7.87 (m, 2H), 7.74(d, J = 8.8 Hz, 1H), 7.69–7.64 (m, 2H), 7.44–7.42 (m, 2H), 7.17 (m, 1H), 7.09 (d, J = 4 Hz, 2H), 4.42–4.40 (m, 2H), 3.8 (s, 6H), 3.75 (s, 3H), 1.25–1.20 (m, 3H); ^{13}C NMR (100 MHz, DMSO-d_6): δ 153.60, 144.13, 140.69, 139.03, 135.55, 131.21, 130.33, 128.58, 126.93, 125.32, 122.97, 121.12, 119.59, 119.29, 112.55, 111.73, 106.07, 60.69, 56.51, 40.62, 15.12; HRMS: for $C_{26}H_{25}N_3O_3$, Exact Mass: 427.1896; observed $[M + H]^+$: 428.1967.

4-ethyl-1-(4-fluorophenyl)-3-(4-methoxyphenyl)-1,4-dihydropyrazolo[4,3-*b*]indole (**7f**)

Compound **7f** was synthesized in accordance with the typical procedure discussed above. Purification by column chromatography on silica gel (PE/A = 99:1) afforded **7f** (22%) as a cream solid; mp: 158–159 °C; ^{1}H NMR (400 MHz, DMSO-d_6) δ 7.90–7.87 (m, 2H), 7.80 (d, J = 8.1 Hz, 1H), 7.71 (d, J = 8.5 Hz, 2H), 7.62 (d, J = 8.4 Hz, 1H), 7.44 (t, J = 8.7 Hz, 3H), 7.14 – 7.07 (m, 3H), 4.34–4.29 (m, J = 7.0 Hz, 2H), 3.81 (s, 3H), 1.07 (m, 3H). ^{13}C NMR (100 MHz, DMSO-d_6) δ 161.91, 159.78, 144.20, 137.32, 135.43, 131.28, 131.07, 130.10, 125.25, 122.99, 122.91, 119.50, 119.25, 117.22, 116.99, 114.71, 112.57, 111.72, 55.73, 40.65, 15.00.

1-(2,4-dichlorophenyl)-4-ethyl-3-(4-methoxyphenyl)-1,4-dihydropyrazolo[4,3-*b*]indole (**7 g**)

Compound **7 g** was synthesized in accordance with the typical procedure discussed above. Purification by column chromatography on silica gel (PE/A = 99:1) afforded **7 g** (22%) as a cream solid; mp: 124–125 °C; ^{1}H NMR (400 MHz, DMSO-d_6) δ 7.94 (d, J = 2.2 Hz, 1H), 7.76 – 7.58 (m, 5H), 7.34–7.31 (m, 2H), 7.09 – 7.02 (m, 3H), 4.35–4.30

(m, 2H), 3.8(s, 3H), 1.12–1.08 (m, 3H). ^{13}C NMR (100 MHz, DMSO-d_6) δ 159.81, 144.04, 137.26, 135.93, 133.96, 133.77, 130.82, 130.23, 130.08, 129.99, 129.20, 125.19, 125.14, 119.38, 119.23, 114.74, 112.65, 111.54, 55.73, 39.49, 15.20.

4-ethyl-3-(3-iodo-4-methoxyphenyl)-1-phenyl-1,4-dihydropyrazolo [4,3-*b*]indole (**7i**)

Compound **7i** was synthesized in accordance with the typical procedure discussed above. Purification by column chromatography on silica gel (PE/A = 99:1) afforded **7i** (41%) as a cream solid; mp: 173–175 °C; ^{1}H NMR (400 MHz, DMSO-d_6): δ 8.16–8.18 (m, 1H), 7.94 (d, J = 8.6 Hz, 1H), 7.88 – 7.77 (m, 3H), 7.69 (d, J = 8.6 Hz, 1H), 7.64 – 7.59 (m, 2H), 7.38 (t, J = 7.0 Hz, 2H), 7.16–7.11 (m, 2H), 4.32–4.28 (m, 2H), 3.88 (s, 3H), 1.13–1.08 (m, 3H); ^{13}C NMR (100 MHz, DMSO-d_6): δ 158.36, 144.22, 140.30, 139.01, 138.93, 134.34, 130.33, 130.15, 127.03, 125.48, 122.94, 121.06, 119.79, 119.62, 112.53, 112.11, 111.73, 91.54, 86.95, 57.06, 40.67, 15.05; HRMS: for $C_{24}H_{20}IN_3O$, Exact Mass: 493.0651; observed $[M + H]^+$: 494.0714.

4-ethyl-3-(naphthalen-2-yl)-1-phenyl-1,4-dihydropyrazolo[4,3-*b*] indole (**7j**)

Compound **7j** was synthesized in accordance with the typical procedure discussed above. Purification by column chromatography on silica gel (PE/A = 99:1) afforded **7j** (48%) as a white solid; mp: 177–179 °C; ^{1}H NMR (400 MHz, DMSO-d_6): δ 8.34 (s, 1H), 8.07–8.04 (m, 2H), 7.99 – 7.92 (m, 4H), 7.90–7.86 (m, 1H), 7.75 (d, J = 8.7 Hz, 1H), 7.69–7.62 (m, 2H), 7.58 – 7.53 (m, 2H), 7.42–7.38 (m, 2H), 7.18–7.14 (m, 1H), 4.44 – 4.41 (m, 2H), 1.10–1.05 (m, 3H). ^{13}C NMR (100 MHz, DMSO-d_6): δ 144.40, 140.70, 139.06, 133.51, 133.04, 131.53, 130.49, 130.36, 128.83, 128.70, 128.25, 127.60, 127.50, 127.20, 127.01, 126.79, 125.41, 122.99, 121.13, 119.64, 119.41, 112.72, 111.82, 40.62, 15.02; HRMS: for $C_{22}H_{21}N_3$, Exact Mass: 388.1805; observed $[M + H]^+$: 388.1801.

General Procedure for the synthesis of 8d *in-situ* benzylation. To an oven-dried Microwave vial was added **5d** (1 mmol, 1 equiv), PPh_3 (3 equiv), benzyl chloride (1.5 equiv) and toluene (5 mL). The mixture was stirred at 180 °C in the CEM (sealed tube) for 20 min. After TLC indicated that **5d** was completely consumed. Toluene was evaporated under vaccum, and the mixture was poured in water and extracted with ethyl acetate (25 mL). Then the solvent was evaporated under vacuum. The crude product was purified using flash column chromatography (eluent: Petroleum ether/Acetone) on silica gel to afford the desired product **8d**. Cream solid; Purification by column chromatography on silica gel (PE/A = 19:1): 61% yield; mp: 140–142 °C: ^{1}H NMR (500 MHz, DMSO-d_6): δ 7.92–7.95 (m, 3H), 7.69–7.64 (m, 5H), 7.45 – 7.38 (m, 2H), 7.20 (d, J = 8.6 Hz, 4H), 7.04 (d, J = 10.4 Hz, 2H), 6.94 (d, J = 8.5 Hz, 2H), 5.56 (s, 2H), 3.82 (s, 3H); ^{13}C NMR (125 MHz, DMSO-d_6): δ 159.74, 144.71, 140.66, 138.12, 135.43, 131.62, 131.24, 130.27, 130.15, 129.07, 127.78, 126.78, 126.76, 125.38, 125.05, 120.91, 119.63, 119.62, 114.62, 112.87, 112.17, 55.69, 47.75; HRMS: for $C_{29}H_{23}N_3O$, Exact Mass: 429.1841; observed $[M + H]^+$: 430.1920.

Procedure for controlled experiments. To gather more pieces of evidence in favor of the nitrene pathway, we set a controlled experiment (Scheme S2) where a reaction of **5d** (1 equiv) with triethyl phosphite (3 equiv) was carried out in toluene as solvent. The reaction mixture was refluxed for 4 h, and the sample was collected from the reaction mixture for LCMS analysis.

5. Biology

5.1. Cell lines and cell culture

Cell lines (MDA-MB-231, MCF-7, A549, and HCT-116) were procured from National Centre for Cell Science (NCCS) Pune, India and maintained per instructions in DMEM media mixed with 10% FBS, 1% Penicillin-Streptomycin solution in a CO_2 incubator. Upon reaching 80% confluency, they were passaged with the help of 0.25% Trypsin-EDTA solution (Gibco) and were further utilized according to the experimental setup.

Human peripheral blood mononuclear cells (hPBMCs) were isolated from healthy individuals. RBCs were lysed in lysis buffer, and the hPBMCs were cultured in RPMI media and treated accordingly with the compounds as discussed below to assess the selectivity of investigational compounds toward cancer cells. The assay was performed strictly as per protocol no. CUPB/cc/14/IEC/4483 approved by Institutional Ethics Committee of Central University of Punjab, Bathinda, and according to the Indian Council of Medical Research (ICMR) guidelines Govt. of India.

5.2. Evaluation of antiproliferative potential of synthesized compounds by 3-(4,5-dimethythiazol-2-yl)-2,5-diphenyl tetrazolium bromide (MTT) assay

The antiproliferative potential of the investigational compounds was assessed using MTT assay (Invitrogen) in different cells. 7×10^3 cells were seeded in a 96-well plate. The following day, cells were serum-starved, and synthetic compounds were treated and incubated for 24 h following which 10 μL of MTT dye (5 mg/mL of 1X PBS) was added to each well and incubated in CO_2 atmosphere in the dark for 4 h to allow formazan crystals formation. 100 μL DMSO (100%) was added to each well, and absorbance was read using a microplate reader at 570 nm. % cell viability was calculated using the formula given below, and IC_{50} values were calculated using ORIGIN software.

$$\%\ \text{Cell Viability} = \text{OD}_{\text{Test Compound}} / \text{OD}_{\text{Media (Control)}} * 100$$

5.3. Topoisomerase assay

Topoisomerase I (Catalogue No TG2005H-RC) and Topoisomerase II (Catalogue No TG2000H-1) assay kits were procured from Topogen (Topogen, Inc. Buena Vista, CO, USA). DNA relaxation and DNA decatenation assays were performed as per the manufacturer's instructions. Negatively supercoiled DNA (SC DNA) and camptothecin (CPT) were used as substrate and positive control. The total reaction mixture was incubated at 37 ° C for 30 min and stopped by the addition of 2 μL 10% SDS. The samples were run on 0.8% agarose gel for 1–2 h at 50 V and then stained with the help of EtBr for 15 min followed by destaining in water, and images were recorded in Chemi-Doc™ XRS+ (Bio-Rad). For topoisomerase-II, kinetoplast DNA (kDNA) acted as substrate and etoposide, an inhibitor of Topo II, was used as a positive control as described previously.[47]

5.4. Molecular docking studies

The ligand-bound crystal structures of human topoisomerase I and II (PDB ID's: 1T8I [48] and 4R1F [49]) were imported from Protein Data Bank (www.rcsb.org) in Schrodinger (2020–4). Both the proteins were prepared using protein preparation wizard in Maestro 12.6. The binding cavity was defined using receptor grid generation, and the grid was generated around the already bound ligand. All the synthesized ligands were drawn using ChemDraw Professional in 2D format and saved in 'sdf' format. All the ligands were prepared using the LIGPREP module in a 3D format using the OPLS3 force field. All the prepared ligands were docked at the topoisomerase I and II binding sites using the GLIDE module in Maestro 12.6. The result revealed the affinity and binding interactions of ligands with the proteins. The docking scores were generated.[50]

5.5. Mitochondrial membrane potential (MMP) and reactive oxygen species (ROS) assay

To assess MMP and ROS level alteration induced by compounds, cells were plated in 100 mm culture dishes and treated with chosen compounds at their respective IC_{50} values for 24 h. The pellets were washed twice with the help of sterile 1X PBS (Gibco). The MMP in MDA-MB-231

cells was monitored using incubation of JC-1 (Life Technologies, Thermo Fisher Scientific), an MMP-sensitive fluorescent dye, with resuspended cell pellet for 30 min at 37 C and analyzed using a flow cytometer (BD Biosciences, San Jose, CA, USA).

Declaration of Competing Interest

The authors declare that they have no known competing financial interests or personal relationships that could have appeared to influence the work reported in this paper.

Acknowledgements

MK thanks the DST-Inspire, New Delhi (IF 180460), for providing the JRF. MK and RK are thankful to Professor R. P. Tiwari, Vice-Chancellor, to support the present work. RK thanks SERB (EMR/2017/002702), Delhi, for financial support. The authors also thank CIL, CUPB, and DST-FIST (for GC-MS) support to the department for data analysis and CIF, BIT Mesra for X-ray diffraction data collection.

Appendix A. Supplementary material

The Supplementary data includes copies of ^{1}H and ^{13}C NMR spectra, HRMS spectra, LCMS spectra, X-ray crystallographic data (Figure S1) and other figures (such as docking images and drug response curves) (S2-S7) and Schemes. Supplementary data to this article can be found online at https://doi.org/10.1016/j.bioorg.2021.105114.

References

[1] M. Kaur, R. Kumar, C-N and N-N bond formation via Reductive Cyclization: Progress in Cadogan/Cadogan-Sundberg Reaction‡, ChemistrySelect 3 (19) (2018) 5330–5340.
[2] S. Sinha, R. Sikari, V. Sinha, U. Jash, S. Das, P. Brandão, S. Demeshko, F. Meyer, B. de Bruin, N.D. Paul, Iron-Catalyzed/Mediated C-N Bond Formation: Competition between Substrate Amination and Ligand Amination, Inorg. Chem. 58 (3) (2019) 1935–1948.
[3] J. Bariwal, E. Van der Eycken, C-N bond forming cross-coupling reactions: an overview, Chem. Soc. Rev. 42 (24) (2013) 9283–9303.
[4] Ali, I., Nadeem Lone, M., A Al-Othman, Z., Al-Warthan, A., Marsin Sanagi, M., Heterocyclic scaffolds: centrality in anticancer drug development, Curr. Drug Targets 16(7) (2015) 711-734.
[5] L. Zou, X. Duan, W. Zhou, H. Zhang, S. Chen, J. Chai, X. Liu, L. Shen, J. Xu, G. Zhang, Electrochemical capacitive performance of free-standing polyindole film and effect of introducing alkyl chain connecting two indoles, J. Mater. Sci.: Mater. Electron. 1–8 (2019).
[6] C. Lamberth, Heterocyclic chemistry in crop protection, Pest Manage. Sci. 69 (10) (2013) 1106–1114.
[7] S. Urgaonkar, J.G. Verkade, Scope and limitations of Pd2 (dba) 3/P (i-BuNCH2CH2) 3N-catalyzed Buchwald− Hartwig amination reactions of aryl chlorides, J. Org. Chem. 69 (26) (2004) 9135–9142.
[8] V. Gracias, J.D. Moore, S.W. Djuric, Sequential Ugi/Heck cyclization strategies for the facile construction of highly functionalized N-heterocyclic scaffolds, Tetrahedron Lett. 45 (2) (2004) 417–420.
[9] T. Rosenau, A. Potthast, J. Roehrling, A. Hofinger, H. Sixta, P. Kosma, A solvent-free and formalin-free Eschweiler-Clarke methylation for amines, Synth. Comm. 32 (3) (2002) 457–466.
[10] Merisor, E., Synthesis of N-neterocycles via intramolecular reductive cyclizations of nitroalkenes, (2008).
[11] Lu, C., Su, Z., Jing, D., Jin, S., Xie, L., Li, L., Zheng, K., Intramolecular Reductive Cyclization of o-Nitroarenes via Biradical Recombination, Org. Lett. (2019).
[12] H. Peng, X. Chen, Y. Chen, Q. He, Y. Xie, C. Yang, Solvent-free synthesis of δ-carbolines/carbazoles from 3-nitro-2-phenylpyridines/2-nitrobiphenyl derivatives using DPPE as a reducing agent, Tetrahedron 67 (32) (2011) 5725–5731.
[13] J.S. Zhu, C.J. Li, K.Y. Tsui, N. Kraemer, J.-H. Son, M.J. Haddadin, D.J. Tantillo, M. J. Kurth, Accessing Multiple Classes of 2H-Indazoles: Mechanistic Implications for the Cadogan and Davis-Beirut Reactions, J. Am. Chem, Soc, 2019.
[14] M. Shevlin, X. Guan, T.G. Driver, Iron-catalyzed reductive cyclization of O-nitrostyrenes using phenylsilane as the terminal reductant, ACS Catalysis 7 (8) (2017) 5518–5522.
[15] P. Bunyan, J. Cadogan, 7. The reactivity of organophosphorus compounds. Part XIV. Deoxygenation of aromatic C-nitroso-compounds by triethyl phosphite and triphenylphosphine: a new cyclization reaction, J. Chem. Soc. (1963) 42–49.
[16] R. Sundberg, Deoxygenation of nitro groups by trivalent phosphorus. Indoles from o-nitrostyrenes, J. Org. Chem. 30 (11) (1965) 3604–3610.
[17] P. Bhutani, G. Joshi, N. Raja, N. Bachhav, P.K. Rajanna, H. Bhutani, A.T. Paul, R. Kumar, US FDA approved drugs from 2015–June 2020: a perspective, J. Med. Chem. 64 (5) (2021) 2339–2381.
[18] C. Sawyers, Targeted cancer therapy, Nature 432 (7015) (2004) 294–297.
[19] J.L. Delgado, C.-M. Hsieh, N.-L. Chan, H. Hiasa, Topoisomerases as anticancer targets, Biochem. J. 475 (2) (2018) 373–398.
[20] M. Westphal, C.L. Maire, K. Lamszus, EGFR as a target for glioblastoma treatment: an unfulfilled promise, CNS drugs 31 (9) (2017) 723–735.
[21] C. Zhao, H. Dong, Q. Xu, Y. Zhang, Histone deacetylase (HDAC) inhibitors in cancer: a patent review (2017-present), Expert Opin. Ther. Pat. 30 (4) (2020) 263–274.
[22] F. You, C. Gao, Topoisomerase inhibitors and targeted delivery in cancer therapy, Curr. Top. Med. Chem. 19 (9) (2019) 713–729.
[23] Y. Wan, Y. Li, C. Yan, M. Yan, Z. Tang, Indole: A privileged scaffold for the design of anti-cancer agents, Eur. J. Med. Chem. 183 (2019), 111691.
[24] N. Chadha, O. Silakari, Indoles: As Multitarget Directed Ligands in Medicinal Chemistry, Elsevier, Key Heterocycle Cores for Designing Multitargeting Molecules, 2018, pp. 285–321.
[25] A.B. Smith, A.H. Davulcu, L. Kürti, Indole Diterpenoid Synthetic Studies. Construction of the Heptacyclic Core of (−)-Nodulisporic Acid D, Org. Lett. 8 (8) (2006) 1669–1672.
[26] N. Chadha, O. Silakari, Indoles as therapeutics of interest in medicinal chemistry: Bird's eye view, Eur. J. Med. Chem. 134 (2017) 159–184.
[27] S. Issa, A. Prandina, N. Bedel, P. Rongved, S. Yous, M. Le Borgne, Z. Bouaziz, Carbazole scaffolds in cancer therapy: a review from 2012 to 2018, J. Enzyme Inhib. Med. Chem. 34 (1) (2019) 1321–1346.
[28] J.M. Alex, R. Kumar, 4, 5-Dihydro-1 H-pyrazole: an indispensable scaffold, J. Enzyme Inhib. Med. Chem. 29 (3) (2014) 427–442.
[29] G. Joshi, S.M. Amrutkar, A.T. Baviskar, H. Kler, S. Singh, U.C. Banerjee, R. Kumar, Synthesis and biological evaluation of new 2, 5-dimethylthiophene/furan based N-acetyl pyrazolines as selective topoisomerase II inhibitors, RSC Adv. 6 (18) (2016) 14880–14892.
[30] S. Kumar, H. Ila, H. Junjappa, Efficient Routes to Pyrazolo [3, 4-b] indoles and Pyrazolo [1, 5-a] benzimidazoles via Palladium-and Copper-Catalyzed Intramolecular C− C and C− N Bond Formation, J. Org. Chem. 74 (18) (2009) 7046–7051.
[31] Z. Hou, S. Oishi, Y. Suzuki, T. Kure, I. Nakanishi, A. Hirasawa, G. Tsujimoto, H. Ohno, N. Fujii, Diversity-oriented synthesis of pyrazolo [4, 3-b] indoles by gold-catalyzed three-component annulation: application to the development of a new class of CK2 inhibitors, Org. Biomol. Chem. 11 (20) (2013) 3288–3296.
[32] H. Liu, L. Zhang, F. Zhao, H. Liu, Three-Step One-Pot Synthesis of 1, 4-Dihydro-pyrazolo [4, 3-b] indoles Using Copper Catalysis, Eur. J. Org. Chem. 2014 (5) (2014) 1047–1052.
[33] J.M. Alex, S. Singh, R. Kumar, 1-Acetyl-3, 5-diaryl-4, 5-dihydro (1H) pyrazoles: exhibiting anticancer activity through intracellular ROS scavenging and the mitochondria-dependent death pathway, Arch. Pharm. 347 (10) (2014) 717–727.
[34] C.O. Kappe, Microwave dielectric heating in synthetic organic chemistry, Chem. Soc. Rev. 37 (6) (2008) 1127–1139.
[35] M. Frisch, G. Trucks, H. Schlegel, G. Scuseria, M. Robb, J. Cheeseman, G. Scalmani, V. Barone, B. Mennucci, G. Petersson, Gaussian 09, Gaussian Inc, Wallingford, CT, 2009.
[36] C. Lee, W. Yang, R. Parr, Density-functional exchange-energy approximation with correct asymptotic behaviour, Phys. Rev. B 37 (1988) 785–789.
[37] C. Lee, W. Yang, R.G. Parr, Development of the Colle-Salvetti correlation-energy formula into a functional of the electron density, Phys. Rev. B 37 (2) (1988) 785.
[38] R.J. Sundberg, T. Yamazaki, Rearrangements and ring expansions during the deoxygenation of. beta., beta.-disubstituted o-nitrostyrenes, J. Org. Chem. 32 (2) (1967) 290–294.
[39] R. Sundberg, A Study of the Deoxygenation of Some o-Alkylnitro-and o-Alkylnitrosobenzenes in Triethyl Phosphite1, J. Am. Chem. Soc. 88 (16) (1966) 3781–3789.
[40] N. Ono, The Nitro-Aldol (Henry) Reaction, The Nitro Group in Organic, Synthesis (2001) 30–69.
[41] G.W. Gribble, Recent developments in indole ring synthesis—methodology and applications, J. Chem. Soc., Perkin Trans 1 (7) (2000) 1045–1075.
[42] H. Majgier-Baranowska, J.D. Williams, B. Li, N.P. Peet, Studies on the mechanism of the Cadogan-Sundberg indole synthesis, Tetrahedron Lett. 53 (35) (2012) 4785–4788.
[43] I.T. Alt, B. Plietker, Iron-Catalyzed Intramolecular C (sp2)− H Amination, Angew. Chemi. 55 (4) (2016) 1519–1522.
[44] I.W. Davies, V.A. Guner, K. Houk, Theoretical evidence for oxygenated intermediates in the reductive cyclization of nitrobenzenes, Org. Lett. 6 (5) (2004) 743–746.
[45] C.R. Reczek, N.S. Chandel, The two faces of reactive oxygen species in cancer, Annu. Rev. Cancer Biol. 1 (2017) 79–98.
[46] S. Marchi, C. Giorgi, J.M. Suski, C. Agnoletto, A. Bononi, M. Bonora, E. De Marchi, S. Missiroli, S. Patergnani, F. Poletti, Mitochondria-ros crosstalk in the control of cell death and aging, J. Signal Transduct. 2012 (2012), 329635.
[47] G. Joshi, S. Kalra, U.P. Yadav, P. Sharma, P.K. Singh, S. Amrutkar, A.J. Ansari, S. Kumar, A. Sharon, S. Sharma, E-pharmacophore guided discovery of pyrazolo [1, 5-c] quinazolines as dual inhibitors of topoisomerase-I and histone deacetylase, Bioorg. Chem. 94 (2020), 103409.

[48] B.L. Staker, M.D. Feese, M. Cushman, Y. Pommier, D. Zembower, L. Stewart, A. B. Burgin, Structures of three classes of anticancer agents bound to the human topoisomerase I– DNA covalent complex, J. Med. Chem. 48 (7) (2005) 2336–2345.
[49] F.V. Stanger, C. Dehio, T. Schirmer, Structure of the N-terminal gyrase B fragment in complex with ADP· P i reveals rigid-body motion induced by ATP hydrolysis, PloS one 9 (9) (2014), e107289.
[50] S. Arora, G. Joshi, S. Kalra, A.A. Wani, P.V. Bharatam, P. Kumar, R. Kumar, Knoevenagel/tandem knoevenagel and michael adducts of cyclohexane-1, 3-dione and aryl aldehydes: synthesis, DFT studies, xanthine oxidase inhibitory potential, and molecular modeling, Acs Omega 4 (3) (2019) 4604–4614.